Single step polyol synthesis of highly stable Pt/C/SiO$_2$ catalysts for use in PEMFCs: effects of pH, temperature and W/EG ratio

Eva Sousa, *Sofia* Delgado, *Tiago* Lagarteira, and *Adélio* Mendes[*]

LEPABE - Laboratory for Process Engineering, Environment, Biotechnology and Energy Faculty of Engineering of the University of Porto, Rua Dr. Roberto Frias, 4200-465 Porto, Portugal

Abstract. Hybrid supports have been proposed as a new alternative to increase the stability of ORR catalysts used in PEMFCs for automotive applications since they are known to be stable under harsh conditions. In this work, Pt nanoparticles were deposited over C/SiO$_2$, via single-step polyol method, to take advantage of the corrosion-resistance properties of silica nanoparticles. In fact, the synthesis parameters, namely, pH, temperature, and glycol concentration had a remarkable impact on the Pt size-distribution, crystallinity, and dispersion over the C/SiO$_2$ supports. A maximum ORR activity and stability was obtained for Pt/C/SiO$_2$ catalysts produced at 1:6 W/EG (v/v). The addition of SiO$_2$ nanoparticles to the carbon structure showed their ability to effectively inhibit support corrosion and Pt nanoparticles detachment and/or growth, with the pH adjustments being critical for obtaining highly stable C/SiO$_2$ supports. Pt/C/SiO$_2$ synthetized under acidic conditions revealed the highest stability when subjected to accelerated stress tests (ASTs), losing only 30 % of the initial electrochemically active surface area (ECSA) of Pt after 4 000 cycles from 0.6 to 1 V (*vs* RHE), whereas the commercial Pt/C revealed > 50 % of ECSA loss.

1 Introduction

Polymer Electrolyte Membrane Fuel Cells (PEMFCs) will be an important choice for the future of the transport sector due to their low operation temperature, high power density and cold-start withstand. PEMFCs are especially suited for trucks, buses, ships, trains and larger cars. However, the main technical challenge for automotive PEMFCs commercialization is the insufficient stability of the cathodic electrodes; usually, Pt-based electrocatalysts supported on carbon materials [1]. The reason for not meeting durability targets set by the US Department of Energy (DoE; 5 000 h; 0.44 A·mg^{-1}$_{Pt}$ and < 40 % loss in mass activity after 30 000 cycles) has been assigned to the carbon corrosion and insufficient anchoring strength of the active sites, resulting in Pt nanoparticles growth in size due to coalescence and dissolution/agglomeration or in Pt detachment from the support [2]. Hence, the development of robust and stable supports is a priority in the design of new electrocatalysts for mobile applications.

Despite their poor conductivity and low surface area, the use of metal oxides - such as SnO$_2$ [3], TiO$_2$ [4], Nb$_2$O$_5$ [5] or SiO$_2$ [6] - as supports has attracted special attention since they are known to be stable under highly acidic pH and humidified media. In fact, the addition of metal oxide nanoparticles to the carbon support is a promising pathway to increase the stability of Pt-based electrocatalysts [7]. These hybrid supports are able to keep the carbon structure main properties – porosity and high surface area, conductivity, anchoring sites – while the corrosion-resistance is provided by the metal oxide.

Particularly, Pt/C/SiO$_2$ electrocatalysts have been prepared by covering Pt/C with thin silica layers, using silicon alkoxides (MTEOS, TEOS, APTES, among others) as precursors [8]. The presence of hydrophilic silanol groups (Si-OH) in the final silica layers improves the catalyst wettability, allowing operation at higher current densities due to lower mass-transport overpotentials [9]. However, these electrocatalysts should be carefully prepared since the coverage of the whole surface of Pt/C with thick silica layers might lower its electrical conductivity, leading to insufficient ORR performance.

In this work, Pt/C/SiO$_2$ electrocatalysts were prepared by performing a single step polyol method. Instead of using silicon alkoxides to obtain a silica coating, this new approach considers the addition of SiO$_2$ as a binding element between carbon and Pt nanoparticles. Hence, SiO$_2$ nanoparticles were directly added to the support, avoiding the insulating effect produced by the hydrolysis of silicon precursors. Moreover, the polyol reduction temperature (which depends of the glycol concentration on water) and the pH of the polyol solution are parameters that deeply impact electrocatalysts performance and stability [10,11]. This study reports for the first time the effects of these key synthesis conditions on Pt/C/SiO$_2$ catalysts. The as-prepared catalysts were analyzed with ICP-OES, TGA, TEM, XRD, BET and XPS. Furthermore, their corrosion-resistance was studied performing accelerated stress tests

---

[*] Corresponding author: mendes@fe.up.pt

(ASTs) by cycling the potential between 0.6 and 1.0 V (*vs* RHE) during 4000 cycles.

2 Experimental Section

2.1. Pt/C/SiO₂ synthesis by single step polyol method

The prepared platinum-based catalysts (40 wt.%) supported on carbon-silica materials were denoted as Pt/C/SiO₂. Initially, the support nanoparticles - 16 mg of SiO₂ (Sigma Aldrich) and 30 mg of carbon (Ketjenblack EC-600J from Tanaka) - were dissolved in an aqueous solution of ethane-1,2-diol (EG; VWR Chemicals) and blended for 6 h. The platinum precursor, $H_2PtCl_6 \cdot 6H_2O$ (Sigma Aldrich) was added to the support nanoparticles and stirred during 12 h. After the pH adjustment, the synthesis was performed at the boiling point of the colloidal solution for 6 h under continuous stirring. Lastly, after the reacting mixture reached room temperature, the obtained powder was filtered and washed with MilliQ-water several times; the electrocatalyst was collected and dried at 100 ºC overnight [12]. The electrocatalysts were produced under different glycol concentrations, namely 1:4 Water/EG (W/EG), 1:6 and 1:8 (v/v), which also changed the temperature of the reduction process. The pH was adjusted to produce catalysts at acidic pH=2, alkaline pH=10 and sequential pH=10 to pH=2 (defined as alkaline-acidic medium; the pH was adjusted to alkaline before the synthesis using NaOH (Alfa Aesar) and at the end of the reaction was set again to pH=2, using $H_2SO_{4(aq)}$ (VWR Chemicals)) [13].

For a real assessment, a Pt/C without silica produced under similar conditions and a commercial 40 wt.% Pt/Ketjenblack (Premetek) were used as benchmark catalysts.

2.2 Electrochemical Measurements

A three-electrode configuration was prepared using a Rotating Disk Electrode (RDE) from Pine Research Instrumentation. For that, a carbon rod was used as a counter electrode, a saturated Ag/AgCl in 3 M $KCl_{(aq)}$ as reference electrode, and a glassy carbon surface (GCE, 0.196 cm²) as working electrode. A small quantity of catalyst powder (5 mg) was dispersed using a 1:4 (v/v) isopropanol/water solution; 20 μL were further dropped onto the GCE and dried at 700 rpm and 25 °C. A potentiostat - Zahner IM6-ex - was used to perform the electrochemical measurements. Firstly, the working electrode was activated by cycling the potential between 50 mV and 1 V (*vs* RHE) at 100 mV·s⁻¹ during 100 cycles under inert atmosphere. The ohmic resistance of the electrolyte - 0.1 M $HClO_{4(aq)}$ (70 % conc. Sigma Aldrich) - was obtained by performing electrochemical impedance spectroscopy (EIS) at 0.4 V *vs* RHE using a small amplitude perturbation of 5 mV at 1 kHz. Cyclic voltammograms (CVs) were obtained under Ar-saturated 0.1 M $HClO_{4(aq)}$ at 25 °C using a scan rate of 20 mV·s⁻¹. The electrochemical surface area (ECSA) was calculated from the hydrogen desorption peaks from 0.05 to 0.4 V (*vs* RHE), assuming a fully hydrogen-covered platinum (111)

monolayer of 210 μC·cm⁻². Linear Sweep Voltammograms (LSVs) were performed in O₂-saturated 0.1 M $HClO_{4(aq)}$ electrolyte at 25 °C. LSVs were obtained from 0.05 to 1 V *vs* RHE at a scan rate of 20 mV·s⁻¹ and 1600 rpm. Background currents were obtained by performing the same test in inert atmosphere - Ar-saturated 0.1 M $HClO_{4(aq)}$ electrolyte. Electrochemical performance was evaluated during ASTs, by cycling the potential between 0.6 and 1.0 V *vs* RHE for 4000 cycles at a scan rate of 100 mV·s⁻¹ in O₂-saturated electrolyte.

3 Results and Discussion

Pt/C/SiO₂ catalysts were extensively analyzed using morphological characterization (including XRD, XPS, BET, ICP, TGA, among others; not shown). These analyses were further correlated with the electrochemical results. As expected, temperature, glycol concentration and pH adjustments generated important differences on the size-distribution, crystallinity, and dispersion of Pt nanoparticles on C/SiO₂ supports, which in turn impacts electrocatalysts ORR performance.

Fig. 1. a) and b) show CVs obtained for the catalysts produced under alkaline-acidic sequence pH and acidic pH, respectively; both exhibited well-shaped peaks of hydrogen adsorption/desorption, which indicates that the silica nanoparticles did not hinder O₂ diffusion to the Pt active sites.
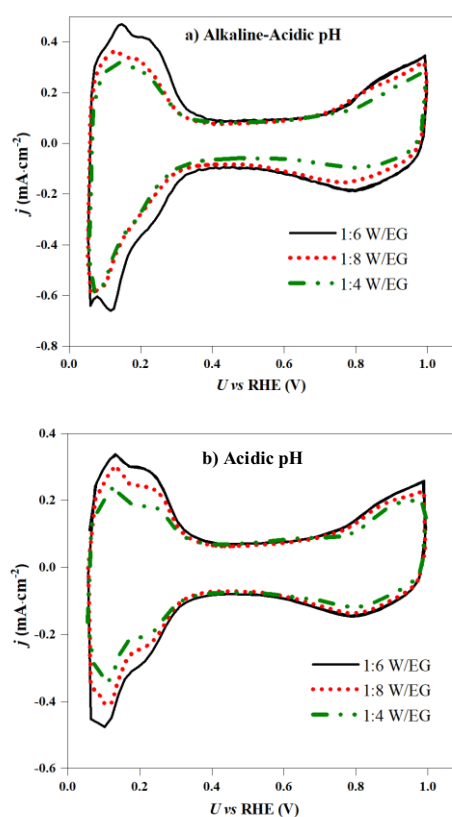

Fig. 1. CVs for a) Pt/C/SiO₂ prepared under 1:4, 1:6, 1:8 W/EG concentration and alkaline-acidic conditions, b) Pt/C/SiO₂ prepared using 1:4, 1:6 and 1:8 W/EG and acidic medium; in Ar-purged 0.1 M HClO₄ electrolyte. Scan rate of 20 mV·s⁻¹.

In fact, the alkaline-acidic pH control delivered catalysts with improved ECSA and ORR mass-activity due to a better dispersion of Pt over the support, as shown in TEM images, **Fig. 2**. During the synthesis under alkaline medium, Pt cations are surrounded by negatively charged acetaldehyde species, which in turn hinders coalescence or agglomeration of Pt precursor; thus, high pH contributes to a better dispersion of the active sites over the support [14]. However, such effect also produces repulsive electrostatic forces between Pt and support nanoparticles, caused by their same electric surface charge. Hence, after carrying out the reaction under alkaline medium, the pH can be changed to acidic, to allow the complete nucleation of Pt on the anchoring sites of the support. The alkaline-acidic process and the acidic pH control allowed a complete utilization of Pt precursor [13]. On the other hand, an incomplete Pt deposition was verified for the electrocatalysts prepared under alkaline pH, thus making the production of these catalysts uncompetitive.
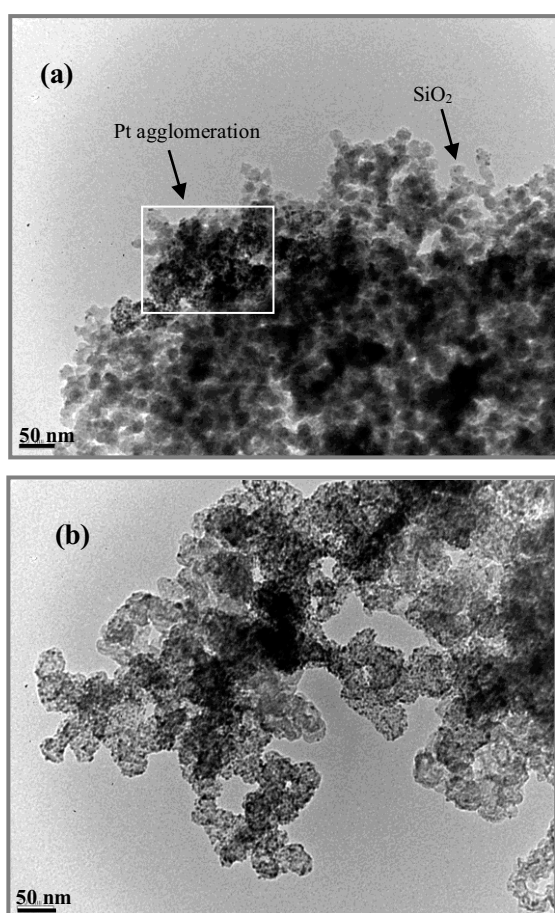

Fig. 2. TEM images of a) 1:8 W/EG Pt/C/SiO$_2$ prepared under acidic conditions; and b) 1:8 W/EG Pt/C/SiO$_2$ prepared using the sequential alkaline-acidic method.

Higher glycol concentration means higher reduction temperature of the polyol process (set by the boiling point of the reaction solution). The faster reduction kinetics under higher temperature delivers smaller Pt nanoparticles, but can also produce agglomerates of individual Pt, which compromises ECSA and ORR mass-activity [15]. **Fig. 3.**

shows that a proportion of 1:6 W/EG results in the highest ECSA and ORR mass-activity, regardless of the pH medium, during Pt/C/SiO$_2$ synthesis. ECSA and ORR mass-activity values of 58.0 m^2·g$_{Pt}^{-1}$ and 83.3 mA·mg$_{Pt}^{-1}$ were achieved for the acidic pH, respectively; and 85.2 m^2·g$_{Pt}^{-1}$ and 93.1 mA·mg$_{Pt}^{-1}$ for the alkaline-acidic 1:6 W/EG Pt/C/SiO$_2$ catalyst. The larger ORR mass-activity at 1:6 W/EG reveals improved mass diffusion pathways and porosity, which provide better access of oxygen to the active sites. Despite the presence of silica nanoparticles, 1:6 Pt/C/SiO$_2$ catalysts reached higher ORR mass-activity than the commercial 40 % Pt/Ketjenblack (65.6 mA·mg$_{Pt}^{-1}$).
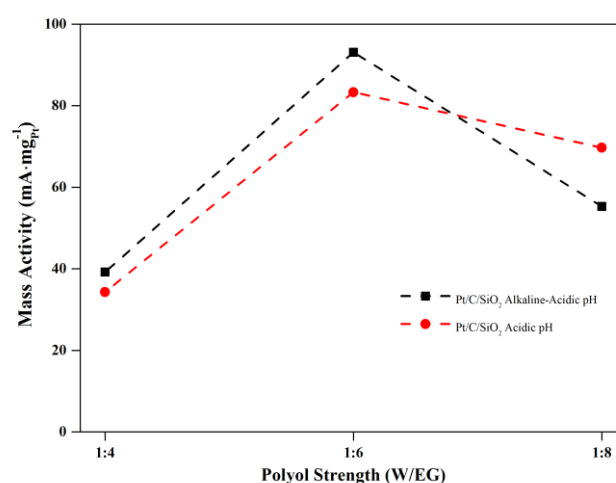

Fig. 3. ORR mass-activity as function of the polyol strength, considering both acidic and alkaline-acidic pH.

Stability of Pt/C/SiO$_2$ catalysts was evaluated by performing potential cycling between 0.6 - 1 V *vs* RHE in O$_2$-saturated 0.1 M HClO$_{4(aq)}$ electrolyte during 4 000 cycles. The acidic Pt/C/SiO$_2$ catalysts revealed the best stability under stress conditions; **Fig. 4.** shows its performance upon degradation.

In detail, silica nanoparticles have silanol groups (Si-OH) at their near-surface, that can change their electric charge according to the pH of the reactive solution [16]. Therefore, during the alkaline-acidic sequence, silica and carbon nanoparticles are initially both negatively charged, which can contribute to a weakened bond between the final C/SiO$_2$ support. The latter can be confirmed by TEM images that revealed silica nanoparticles well incorporated in carbon in the catalysts prepared under acidic pH, but in the alkaline-acidic catalysts, silica is only present in specific regions. Besides, ECSA and mass-activity values upon ageing revealed the poor stability of the alkaline-acidic 1:6 W/EG Pt/C/SiO$_2$ catalyst; its ECSA decreased from 85 to 40 m^2·g$_{pt}^{-1}$ upon 4 000 cycles (53 % loss), **Fig. 5**. Instead, the loss of ECSA of catalysts obtained under acidic pH was inhibited from 58 m^2·g$_{pt}^{-1}$ to 37 m^2·g$_{pt}^{-1}$ (32 % loss). It is evident that C/SiO$_2$ produced under acidic pH promotes a stronger corrosion-resistant behavior. Also, according to its LSV, **Fig. 4.** b), the small loss in the mass transport region suggests a slight modification in the microstructure of the catalyst upon degradation.
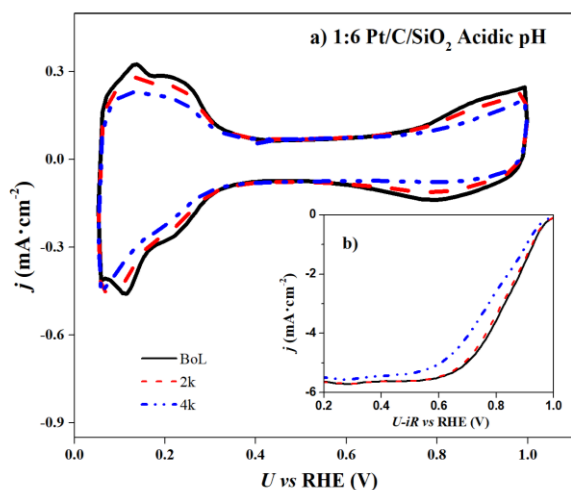
Fig. 4. a) CVs for Pt/C/SiO$_2$ prepared under 1:6 W/EG and acidic medium; in Ar-purged 0.1 M HClO$_4$ electrolyte, before and after ASTs; b) LSVs obtained in O$_2$-purged 0.1 M HClO$_4$ electrolyte. Scan rate of 20 mV·s^{-1}.

The same stability protocol was applied to the 1:6 W/EG Pt/C prepared under similar conditions of pH, glycol concentration and without silica. The electrochemical results were compared with those obtained for the commercial 40 % Pt/Ketjenblack, **Fig. 6**. ECSA for the Pt/C catalyst decreased after 4 000 cycles to 36 m^2·g$_{pt}^{-1}$ (41 % loss); its ORR mass-activity loss was also very significant, almost 70 %, which shows the greatly superior stability of acidic Pt/C/SiO$_2$ - lost only 38 % of its initial mass-activity.
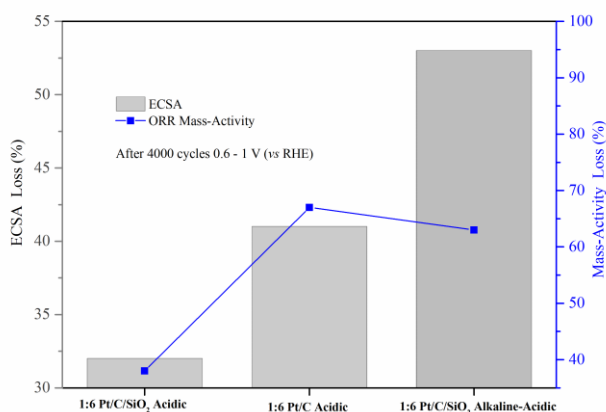

Fig. 5. ORR mass-activity and ECSA of electrocatalysts with and without silica, prepared using 1:6 W/EG, upon ageing.

Typically, Pt nanoparticles detachment or sintering/agglomeration during catalysts degradation significantly contributes to a decrease of the active surface area available for ORR, resulting in substantial losses of ORR mass-activity [2]. It was verified a remarkably higher loss of active surface area in the catalysts without silica. Hence, the addition of SiO$_2$ nanoparticles leads to higher binding strength between carbon and Pt nanoparticles, effectively inhibiting support corrosion and Pt degradation

mechanisms, which might include migration, detachment, and sintering/agglomeration phenomena.
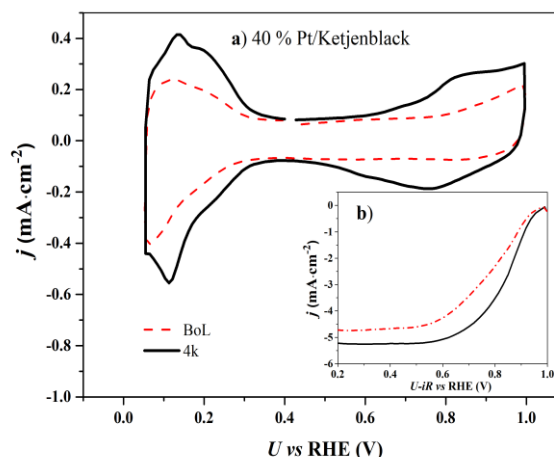

Fig. 6. a) CVs for commercial Pt/C in Ar-purged 0.1 M HClO$_4$ electrolyte, before and after ASTs; b) LSVs obtained in O$_2$-purged 0.1 M HClO$_4$ electrolyte. Scan rate of 20 mV·s^{-1}.

Moreover, the ECSA of the commercial 40 % Pt/Ketjenblack decreased 52 % after 4 000 cycles, confirming the improved stability of acidic Pt/C/SiO$_2$ catalysts at PEMFC cathodic conditions.

4 Conclusion

Pt/C/SiO$_2$ catalysts were successfully produced via single step polyol method. Glycol concentration and pH of polyol solution strongly impacted Pt size-distribution, and its dispersion over C/SiO$_2$ supports. The maximum ORR mass-activity was achieved at 1:6 W/EG (v/v). Moreover, highly stable C/SiO$_2$ supports were obtained under acidic pH conditions, due to favorable electrostatic forces between silica and carbon nanoparticles displayed under such medium. A sequential alkaline-acidic process delivers Pt/C/SiO$_2$ with improved ECSA and ORR mass-activity, but its degradation under stress was significantly higher (> 50 % ECSA losses). Instead, the acidic Pt/C/SiO$_2$ catalysts lost only 30 % of its initial ECSA, with the interactions between carbon and silica enhancing support stability and inhibiting Pt degradation mechanisms.

Acknowledgments

References

1. B. G. Pollet, S. S. Kocha, and I. Staffell, Curr. Opin. Electrochem. **16**, 90 (2019)

2. E. Padgett, V. Yarlagadda, M. E. Holtz, M. Ko, B. D. A. Levin, R. S. Kukreja, J. M. Ziegelbauer, R. N. Andrews, J. Ilavsky, A. Kongkanand, and D. A. Muller, J. Electrochem. Soc. **166**, F198 (2019)

3. G. Cognard, G. Ozouf, C. Beauger, L. Dubau, M. López-Haro, M. Chatenet, and F. Maillard, Electrochim. Acta **245**, 993 (2017)

4. Y. Dai, B. Lim, Y. Yang, C. M. Cobley, W. Li, E. C. Cho, B. Grayson, P. T. Fanson, C. T. Campbell, Y. Sun, and Y. Xia, Angew. Chemie - Int. Ed. **49**, 8165 (2010)

5. A. Ishihara, C. Wu, T. Nagai, K. Ohara, K. Nakada, K. Matsuzawa, T. Napporn, M. Arao, Y. Kuroda, S. Tominaka, S. Mitsushima, H. Imai, and K. ichiro Ota, Electrochim. Acta **283**, 1779 (2018)

6. S. Takenaka, D. Mikami, E. Tanabe, H. Matsune, and M. Kishida, Appl. Catal. A Gen. **492**, 60 (2015)

7. E. Antolini and E. R. Gonzalez, Solid State Ionics **180**, 746 (2009)

8. S. Takenaka, R. Akiyama, I. T. Kim, H. Matsune, and M. Kishida, Chem. Lett. **46**, 851 (2017)

9. S. Takenaka, H. Miyamoto, Y. Utsunomiya, H. Matsune, and M. Kishida, J. Phys. Chem. C **118**, 774 (2014)

10. X. Li and I. M. Hsing, Electrochim. Acta **51**, 5250 (2006)

11. C. C. Chou, C. H. Liu, and B. H. Chen, Energy **70**, 231 (2014)

12. P. Dhanasekaran, A. Shukla, S. V. Selvaganesh, S. Mohan, and S. D. Bhat, J. Power Sources **438**, (2019)

13. H. S. Oh, J. G. Oh, and H. Kim, J. Power Sources **183**, 600 (2008)

14. L. Pak Hoe, M. Boaventura, T. Lagarteira, L. Kee Shyuan, and A. Mendes, Int. J. Hydrogen Energy 1 (2018)

15. L. S. and G. V. F. Fievet, S. Ammar-Merah, R. Brayner, F. Chau, M. Giraud, F. Mammeri, J. Peron, J.-Y. Piquemal, (2018)

16. J. Cloarec, J. Genest, J. Beauvais, and H. Chamas, (2014)